

THERMAL CONDUCTANCE  
OF TWO-DIMENSIONAL CONSTRICTIONS

by

T. Nejat Veziroglu, Professor

and

Suresh Chandra, Assistant Professor  
Mechanical Engineering Department  
University of Miami  
Coral Gables, Florida

Abstract

A theoretical and experimental investigation of thermal conductance of two-dimensional constrictions has been carried out for both symmetrical and eccentric constrictions. Analytical solutions for both of these cases have been obtained. The solutions have been presented in terms of dimensionless numbers - a conductance number and a constriction number for the symmetrical case, and additionally an eccentricity number for the eccentric case. A series of experiments have been run by making use of the electrical analogy. Good agreement has been found between the theories and experiments. The results have also been compared with previously reported experiments and theories.

Introduction

When heat flows through a constriction, a thermal resistance (or conductance) develops because of the con-

vergence and divergence of the flow lines at and near the constriction. This resistance is usually quite high compared to the resistance offered to heat flow away from the constriction. For a reliable heat transfer analysis of a given system, such constriction resistances must be accurately predicted in addition to other parameters. Especially, as need for more dependable systems grows in aerospace, nuclear and other industries, it is becoming increasingly necessary for designers to be able to predict the thermal constriction resistances or conductances with greater accuracy. Thermal conductance of three dimensional constrictions has been extensively investigated, presumably because of the fact that it arises in the thermal conductance of contacts - a subject which has received wide attention<sup>(1,2,3)</sup> in the last twenty years. In contrast, the problem of the thermal conductance of two-dimensional constrictions has received little attention. Kouwenhoven and Sackett<sup>(4,5)</sup> carried out an experimental and theoretical study of electrical constriction resistances. Using a simplified model they derived a relationship - containing an experimentally determined parameter - for the symmetrical two-dimensional constriction resistances, and also a relationship for the percentage increase in resistances of eccentric constrictions. Mikic and Rohsenow<sup>(6)</sup> obtained theoretical expressions, in the form of infinite series, for symmetrical two-dimensional constriction resistances for two different heat flux distributions at the constriction. In practice, the two-dimensional constriction

conductance arises in heat transfer at fin bases, in heating a material by means of an electric resistance, in cooling a wall by means of a fluid circulating in tubes (see Figure 1), and in similar situations wherever the constriction is two-dimensional. It even arises in thermal contact conductances when one of the contact surfaces has a two-dimensional roughness and the other is relatively smooth.

The present work provides a theoretical and experimental study of the subject for both symmetrical and eccentric constrictions. The solutions are expressed in terms of dimensionless numbers. The results are compared with the previously reported experimental data and theories.

### Theory

First a solution for the thermal conductance of two-dimensional constrictions will be obtained for the symmetrical case, i.e., when the symmetry axes of both the heat channel and the constriction coincide, and then the eccentric case will be studied.

#### Symmetrical Constriction

Fig. 2 shows the steady state isotherms and heat flow lines for a two-dimensional symmetrical constriction. The heat flow channel width is  $2a$ , the constriction width  $2b$ , and the channel thickness  $t$ . Because of the symmetry, it will suffice to consider only one of the quarter planes, e.g., the one bounded by positive  $x$  and positive  $y$  axes. The steady state temperature distribution must satisfy the

Laplace's equation,

$$\frac{\partial^2 T}{\partial x^2} + \frac{\partial^2 T}{\partial y^2} = 0 \quad \dots\dots\dots (1)$$

and the following boundary conditions,

$$\left. \begin{aligned} \left(\frac{\partial T}{\partial x}\right)_{x=0} &= 0 & 0 < y < \infty \\ \left(\frac{\partial T}{\partial x}\right)_{x=a} &= 0 & 0 < y < \infty \\ \left(\frac{\partial T}{\partial y}\right)_{y=0} &= 0 & b < x < a \\ (T)_{y=0} &= \text{Constant} & 0 < x < b \end{aligned} \right\} \dots\dots\dots (2)$$

The temperature distribution satisfying equation (1) and the conditions (2) can be obtained from a very simple, linear, temperature distribution by means of two conformal transformations. Fig. 3 illustrates these transformations. Consider the quarter flow channel having no constriction and bounded by  $X = 0$ ,  $X = a$ , and  $Y = 0$  lines in the complex  $Z$  plane (Fig. 3a). For heat flow along the channel, the steady state temperature distribution is given by

$$T = mY \quad \dots\dots\dots (3)$$

where  $m$  is a constant. Equation (3) satisfies the Laplace's equation and the boundary conditions of,

$$\left. \begin{aligned} \left(\frac{\partial T}{\partial x}\right)_{x=0} &= 0 & 0 < Y < \infty \text{ or along OP} \\ \left(\frac{\partial T}{\partial x}\right)_{x=a} &= 0 & 0 < Y < \infty \text{ or along QR} \\ (T)_{y=0} &= 0 \text{ (Constant)} & 0 < X < a \text{ or along OQ} \end{aligned} \right\} \dots\dots\dots (4)$$

The constant temperature along X axis has been taken as zero for convenience.

The region POQR of the complex Z plane can be transformed into the region POQR of the complex w plane (see Fig. 3b) by means of the conformal transformation of,

$$w = b \sin\left(\frac{\pi Z}{2a}\right) \dots\dots\dots (5)$$

which preserves the Laplace's relationship and the boundary conditions along the transformed boundaries. Writing  $Z = X + iY$  and  $w = u + iv$  in the transformation relationship (5) and considering the real and imaginary terms, one obtains,

$$u = b \sin\left(\frac{\pi X}{2a}\right) \cosh\left(\frac{\pi Y}{2a}\right) \dots\dots\dots (6)$$

and 
$$v = b \cos\left(\frac{\pi X}{2a}\right) \sinh\left(\frac{\pi Y}{2a}\right) \dots\dots\dots (7)$$

Eliminating X between equations (6) and (7) and solving for Y,

$$Y = \frac{a}{\pi} \cosh^{-1} \left\{ \frac{u^2 + v^2 \pm \sqrt{(u^2 + v^2 - b^2)^2 + 4b^2 v^2}}{b^2} \right\} \dots\dots\dots (8)$$

Substituting equation (8) in (3), the temperature distribution T in the transformed region becomes,

$$T = \frac{ma}{\pi} \cosh^{-1} \left\{ \frac{u^2 + v^2 \pm \sqrt{(u^2 + v^2 - b^2)^2 + 4b^2 v^2}}{b^2} \right\} \dots\dots\dots (9)$$

Now the region POQR of the complex w plane can be transformed into the region PQSR of the complex z plane (see Fig. 3c) by means of the conformal transformation of,

$$w = b \frac{\sin\left(\frac{\pi z}{2a}\right)}{\sin\left(\frac{\pi b}{2a}\right)} \dots\dots\dots (10)$$

which also preserves the Laplace's relationship and the boundary conditions along the transformed boundaries. The transformed boundaries and the boundary conditions are exactly those of the original problem posed. From equation (10), the following transformation relationships for the co-ordinates are obtained,

$$u = \frac{b}{\sin(\frac{\pi b}{2a})} \sin(\frac{\pi x}{2a}) \cosh(\frac{\pi y}{2a}) \dots\dots\dots (11)$$

$$v = \frac{b}{\sin(\frac{\pi b}{2a})} \cos(\frac{\pi x}{2a}) \sinh(\frac{\pi y}{2a}) \dots\dots\dots (12)$$

Substituting equations (11) and (12) in (9), and writing the trigonometric and hyperbolic functions in terms of double angles or arguments, the steady state temperature distribution in a constant width flow channel with a symmetrical constriction becomes,

$$T = \frac{ma}{\pi} \cosh^{-1} \left\{ - \frac{\cos(\frac{\pi x}{a}) - \cosh(\frac{\pi y}{a})}{1 - \cos(\frac{\pi b}{a})} \right. \\ \left. \pm \sqrt{\frac{\cos^2(\frac{\pi b}{a}) + \cos^2(\frac{\pi x}{a}) + \cosh^2(\frac{\pi y}{a}) - 2\cos(\frac{\pi b}{a})\cos(\frac{\pi x}{a})\cosh(\frac{\pi y}{a}) - 1}{1 - \cos(\frac{\pi b}{a})}} \right\} \quad (13)$$

The thermal resistance introduced as a result of the constriction in the heat flow channel can be defined as,

$$R_c = \frac{\Delta T_c}{H} \dots\dots\dots (14)$$

where  $\Delta T_c$  is the additional temperature drop produced by the constriction and H the heat flow rate in the channel. The temperature drop  $\Delta T_c$  can be calculated from,

$$\Delta T_c = \lim_{y \rightarrow \infty} \left\{ T - y \frac{\partial T}{\partial y} \right\} \dots \dots \dots (15)$$

In this equation the first term within the brackets represents the actual temperature drop between  $y=\infty$  and  $y=0$  (constriction) and the second term the temperature drop between the same two points if there were no constriction. Substituting equation (13) in (15) and taking the limit, the constriction temperature drop becomes,

$$\Delta T_c = \frac{2am}{\pi} \ln \left\{ \frac{1}{\sin(\frac{\pi b}{2a})} \right\} \dots \dots \dots (16)$$

The heat flow rate H can be calculated from,

$$H = (\text{channel C. S. A.}) (\text{Thermal Conductivity}) \left( \frac{\partial T}{\partial y} \right)_{y=\infty}$$

or  $H = 2at k \left( \frac{\partial T}{\partial y} \right)_{y=\infty} \dots \dots \dots (17)$

From equation (13), the temperature slope at  $y=\infty$  is,

$$\left( \frac{\partial T}{\partial y} \right)_{y=\infty} = m \dots \dots \dots (18)$$

Substituting equation (18) in (17), the heat flow rate becomes,

$$H = 2amtk \dots \dots \dots (19)$$

Substituting equations (16) and (19) in (14), the thermal constriction resistance (for one side of the constriction) is found to be,

$$R_c = \frac{1}{\pi kt} \ln \left\{ \frac{1}{\sin(\frac{\pi b}{2a})} \right\} \dots \dots \dots (20)$$

The constriction conductance per unit area of the flow channel, by definition, is,

$$u = \frac{1}{(\text{Channel C.S.A.}) R_c}$$

or

$$u = \frac{\pi k}{2a \ln \left\{ \frac{1}{\sin \left( \frac{\pi b}{2a} \right)} \right\}} \dots\dots\dots (21)$$

This result can be reduced to a relationship between two dimensionless numbers. Defining a constriction conductance number  $U$  and a constriction number  $C$  as,

$$U = \frac{u \text{ (Channel width)}}{k} = \frac{2au}{k} \dots\dots\dots (22)$$

and

$$C = \frac{\text{Constriction Width}}{\text{Channel Width}} = \frac{2b}{2a} = \frac{b}{a} \dots\dots\dots (23)$$

and combining equations (22) and (23) with (21), the following relationship is obtained,

$$U = \frac{\pi}{\ln \left\{ \frac{1}{\sin \left( \frac{\pi C}{2} \right)} \right\}} \dots\dots\dots (24)$$

### Eccentric Constrictions

Fig. 4 shows a two-dimensional eccentric constriction. The dimensions of the heat flow channel are the same as those of the symmetrical case, except for the new dimension of eccentricity  $e$ , the distance between the center-line of the heat flow channel and the center-line of the constriction. In this case, the steady state temperature distribution must satisfy the Laplace's equation and the following boundary conditions for the cartesian co-ordinate system geometry selected,

$$\left( \frac{\partial T}{\partial x} \right)_{x=0} = 0 \quad 0 < y < \infty \dots\dots\dots (25)$$

$$\left( \frac{\partial T}{\partial x} \right)_{x=2a} = 0 \quad 0 < y < \infty \dots\dots\dots (26)$$

$$\left(\frac{\partial T}{\partial y}\right)_{y=0} = 0 \quad a+e+b < x < a+e-b \quad \dots\dots\dots (27)$$

$$(T)_{y=0} = \text{Constant} \quad a+e-b < x < a+e+b \quad \dots\dots\dots (28)$$

The temperature distribution which satisfies the Laplace's equation and the boundary conditions (25) and (26) is given by,

$$T = my + \sum_{n=1}^{\infty} B_n \exp\left(-\frac{n\pi y}{2a}\right) \cos\left(\frac{n\pi x}{2a}\right) \quad \dots\dots\dots (29)$$

where  $m$  is the temperature slope at  $y=\infty$  and  $B_n$  a constant, dependent on the number  $n$ . It is difficult to satisfy mixed boundary conditions, such as given by equations (27) and (28), a temperature slope condition and a temperature condition respectively. In order to overcome this difficulty, the temperature boundary condition (28) will be replaced by a temperature slope boundary condition, in a way similar to that used by Mikic and Rohsenow<sup>(6)</sup> for the symmetrical constrictions. If  $q$  is the flux along the constriction in the negative  $y$  direction, the new boundary condition, replacing condition (28), becomes,

$$\left(\frac{\partial T}{\partial y}\right)_{y=0} = \frac{q}{k} \quad a+e-b < x < a+e+b \quad \dots\dots\dots (30)$$

The temperature slope at  $y=0$  is found from equation (29) to be,

$$\left(\frac{\partial T}{\partial y}\right)_{y=0} = m - \sum_{n=1}^{\infty} \frac{n\pi}{2a} B_n \cos\left(\frac{n\pi x}{2a}\right) \quad \dots\dots\dots (31)$$

In the determination of the constants  $B_n$  satisfying the boundary conditions (27) and (31), both sides of equation (31) are multiplied by  $\cos\left(\frac{n\pi x}{2a}\right)dx$  and integrated from  $x=0$  to

$x=2a$  by substitution of the defined temperature slopes, and the following result is obtained,

$$\int_{a+e-b}^{a+e+b} \frac{q}{k} \cos\left(\frac{n\pi x}{2a}\right) dx = -\frac{n\pi}{2} B_n \quad \dots\dots\dots (32)$$

An assumption of uniform flux distribution over the constriction gives,

$$q = \frac{\text{Heat Flow Rate in Channel}}{\text{Constriction Area}}$$

$$\text{or} \quad q = \frac{2atmk}{2bt} = \frac{amk}{b} \quad \dots\dots\dots (33)$$

Substituting equation (33) in (32) and carrying out the integration, one obtains,

$$B_n = -\frac{8a^2m}{n^2\pi^2b} \sin\left(\frac{n\pi b}{2a}\right) \cos\left[\frac{n\pi}{2a}(a+e)\right] \quad \dots\dots\dots (34)$$

Substituting equation (34) in (29), the temperature distribution becomes,

$$T = my - \sum_{n=1}^{\infty} \frac{8a^2m}{n^2\pi^2b} \sin\left(\frac{n\pi b}{2a}\right) \cos\left[\frac{n\pi}{2a}(a+e)\right] \exp\left(-\frac{n\pi y}{2a}\right) \cos\left(\frac{n\pi x}{2a}\right) \quad (35)$$

The additional temperature drop  $\Delta T_c$  produced as a result of the constriction is given by,

$$\Delta T_c = \text{Limit}_{y \rightarrow 0} \left\{ y \left( \frac{\partial T}{\partial y} \right)_{y=\infty} - T \right\} \quad \dots\dots\dots (36)$$

The apparent discrepancy between this equation and equation (15), for determining the constriction temperature drops, is caused by the fact that in the temperature distribution used in equation (15) the constriction temperature was selected to be constant (zero) whereas in the temperature distribution used in equation (33) the temperatures far away ( $y=\infty$ ) from the constriction

are taken to be invariant with the size and eccentricity of the constriction. Substituting equation (35) in (36) and taking the limit,

$$\Delta T_c = \sum_{n=1}^{\infty} \frac{8a^2 m}{n^2 \pi^2 b^2} \sin\left(\frac{n\pi b}{2a}\right) \cos\left[\frac{n\pi}{2a}(a+e)\right] \cos\left(\frac{n\pi x}{2a}\right) \dots\dots\dots (37)$$

This temperature drop is not constant for a given constriction but a function of the co-ordinate x along the constriction. This is caused by the approximate nature of the constriction flux distribution used in finding the temperature distribution. Consequently, for the evaluation of the thermal constriction conductance, a mean constriction temperature drop  $\Delta T_{cm}$  will be defined as,

$$\Delta T_{cm} = \frac{1}{2b} \int_{a+e-b}^{a+e+b} \Delta T_c dx \dots\dots\dots (38)$$

Substituting equation (37) in (38) and integrating, one obtains,

$$\Delta T_{cm} = \frac{16a^3 m}{n^3 \pi^3 b^2} \sin^2\left(\frac{n\pi b}{2a}\right) \cos^2\left[\frac{n\pi}{2a}(a+e)\right] \dots\dots\dots (39)$$

Considering one side of the constriction, the thermal constriction conductance per unit area of the flow channel is given by,

$$u = \frac{k \left(\frac{\partial T}{\partial y}\right)_{y=\infty}}{\Delta T_{cm}} \dots\dots\dots (40)$$

Substituting equations (35) and (39) in (40),

$$u = \frac{\pi^3 b^2 k}{16a^3 \sum_{n=1}^{\infty} \frac{1}{n^3} \sin^2\left(\frac{n\pi b}{2a}\right) \cos^2\left[\frac{n\pi}{2a}(a+e)\right]} \dots\dots\dots (41)$$

The number of variables in the above equation can be reduced by introducing dimensionless numbers U and C defined earlier, and a new dimensionless number, eccentricity number E, defined

as,

$$E = \frac{e}{a-b} \dots\dots\dots (42)$$

so that E varies between 0 and 1 for a given C. Equation (41) can now be written in dimensionless form by using equations (22), (23) and (42), resulting in the following expression,

$$U = \frac{\pi^3 C^2}{8 \sum_{n=1}^{\infty} \frac{1}{n^3} \sin^2 \left( \frac{n\pi}{2} C \right) \cos^2 \left[ \frac{n\pi}{2} (1+E-EC) \right]} \dots\dots\dots (43)$$

It will be seen later that the actual flux distribution along the constriction is not uniform but a parabolic distribution, and that assumption of a uniform flux distribution - made in obtaining the above relationship - leads to lower constriction conductances. Hence, the above relationship will only be used to obtain the ratio of the conductance number for a given eccentricity to that for zero eccentricity so that the errors introduced by the uniform flux assumption would tend to cancel out. If  $U_0$  is the conductance number for no eccentricity, then the ratio is given by,

$$\frac{U}{U_0} = \frac{U}{U_{E=0}} \dots\dots\dots (44)$$

Substituting equation (43) in (44), the conductance ratio becomes,

$$\frac{U}{U_0} = \frac{\sum_{n=1}^{\infty} \frac{1}{n^3} \sin^2 (n\pi C)}{8 \sum_{n=1}^{\infty} \frac{1}{n^3} \sin^2 \left( \frac{n\pi}{2} C \right) \cos^2 \left[ \frac{n\pi}{2} (1+E-EC) \right]} \dots\dots\dots (45)$$

To calculate the conductance number, the exact solution for  $U_0$  given by equation (24) should be used in connection with

the above equation for more precise results. Thus, one obtains,

$$U = \frac{\pi \sum_{n=1}^{\infty} \frac{1}{n^3} \sin^2(n\pi C)}{8 \ln \left\{ \frac{1}{\sin(\frac{\pi}{2}C)} \right\} \sum_{n=1}^{\infty} \frac{1}{n^3} \sin^2(\frac{n\pi}{2}C) \cos^2 \left[ \frac{n\pi}{2}(1+E-EC) \right]} \quad (46)$$

in preference to equation (43). A study of equation (46) shows that U decreases with increase in E and reaches one-half of the value for the symmetrical case when E has its maximum value of unity.

### Experiments

Two series of experiments - one for the symmetrical constrictions and one for the eccentric constrictions - were carried out by making use of the analogy between heat and electricity flows. With the electrical analogy it was easier to reproduce the boundary conditions of the models used, and also the time required to run the experiments was greatly reduced.

Fig. 5 shows the specimens used in the experiments. They were cut from Teledelto's electrical resistance paper No. L-48, in sizes 2 inches wide and 13 inches long. Constrictions were cut in the middle of the specimens. The specimens for studying the symmetrical constrictions represented one-half of the mathematical model, while the specimens for studying the eccentric constrictions represented the complete mathematical model. The constriction half-width b for symmetrical case was varied between 1/8 inch to 1-7/8 inches in

1/8 inch steps. In specimens with eccentric constrictions the constriction width  $2b$  was constant and equal to 1/4 inch while the eccentricity distance  $e$  was varied between 0 and 7/8 inch in 1/8 inch steps.

The experimental set-up is shown in Fig. 6. It was an electrical circuit for measuring the electrical resistance of the specimens and consisted of a constant voltage D.C. power supply (0-40 VDC, 0-5000mA), a milliammeter (0-10mA), a high sensitivity voltmeter (0-50 V) and a switch. Each specimen was painted at the ends over a length of 1/2 inch with low resistivity silver paint. Then the specimen was connected into the circuit by means of two steel fastening clips with tapering widths as shown in the figure. This arrangement insured a uniform current density over the ends of the specimens. The voltmeter probes were placed 8 inches apart and symmetrically with respect to the constriction.

In tests for studying the symmetrical constrictions, only one specimen was used. It was placed in the circuit without any constriction and a D.C. potential of 20 volts was applied across its ends. The voltmeter and ammeter readings were taken. Then a 1/8 inch cut was made in the middle of the specimen in order to provide a constriction, and a mica insulating sheet was put into the cut to avoid any electrical contact across the cut. The power was subsequently turned on and the readings were recorded. This procedure was repeated for decreasing constriction widths, in steps of 1/8 inch decrease at a time.

In tests for studying the eccentric constrictions,

different specimens had to be used for different eccentricities. They were all cut out from the same piece of resistance paper in order to obtain a degree of uniformity in their properties. In addition to specimens with 1/4 inch constrictions, one specimen was prepared with no constriction. The tests were run as described above.

Using the voltmeter and ammeter readings, the resistance of the specimen between voltmeter probes for each experiment was calculated. Let  $R_0$  be the resistance with no constriction and  $R$  the resistance with constriction. Then, considering only one side of the constriction, the additional resistance due to the presence of constriction is given by,

$$R_C = (R - R_0) / 2 \quad \dots\dots\dots (47)$$

The constriction conductance per unit area of the specimen cross section is,

$$u = \frac{1}{(\text{Specimen C.S.A.}) R_C}$$

or, 
$$u = \frac{2}{A (R - R_0)} \quad \dots\dots\dots (48)$$

The dimensionless constriction conductance number, by definition, becomes,

$$U = 2 u \rho \quad \dots\dots\dots (49)$$

where  $\rho$  is the specimen resistivity. The resistivity  $\rho$  can be calculated from a knowledge of no-constriction resistance as follows,

$$\rho = \frac{AR_O}{L} \dots\dots\dots (50)$$

where L is the distance between the voltmeter probes.

Substituting equations (48) and (50) in (49), the conductance number becomes,

$$U = \frac{4aR_O}{L(R-R_O)} \dots\dots\dots (51)$$

For each test, the conductance and constriction numbers were calculated using equations (51) and (23) respectively, and when applicable the eccentricity number was calculated using equation (42).

### Results and Discussion

The theoretical and experimental results for the symmetrical and eccentric constrictions will be considered separately.

#### Symmetrical Constrictions

The results of the present study, together with those of earlier investigators, are plotted in Fig. 7 as the conductance number U versus the constriction number C. The experimental points are those of the present experiments and those of Kouwenhoven and Sackett<sup>(4)</sup> who used metallic specimens and electrical analogy in their experiments. The length of their constriction was not zero, but had a finite value. In other words, the constriction had a neck. The theoretical curves consist of one obtained by Kouwenhoven and Sackett<sup>(4)</sup> and two by Mikic and Rohsenow<sup>(6)</sup> and the present one. Kouwenhoven and Sackett assumed that only a

wedge-like part (made up of sides starting at constriction edges and extending to flow channel boundaries by making a certain angle  $\theta$  with the constriction plane) of the flow channel near the constriction was effective in conducting "electricity", derived an expression for the wedge resistance in terms of the angle  $\theta$  ( $= \frac{\pi}{2}$  - half wedge angle), and determined the angle  $\theta$  from their experiments for the best fit. It was found to be  $41.3^\circ$ . Mikic and Rohsenow used essentially the same model as the one used in the present study with the exception that they specified the thermal flux distribution at the constriction, and obtained two series expressions for two different flux distributions - a uniform flux distribution and a parabolic flux distribution. If  $H$  is the total heat flow rate in the channel, these two flux distributions can be expressed by the following expressions respectively,

$$q_1 = \frac{H}{2bt} \dots\dots\dots (52)$$

and 
$$q_2 = \frac{H}{\pi \sqrt{b^2 - x^2}} \dots\dots\dots (53)$$

From Fig. 7 it can be seen that the assumption of uniform constriction flux distribution results in lower conductances while the assumption of a parabolic flux distribution given by equation (53) results in higher conductances. In the present theory, the flux distribution at the constriction is not pre-specified. The solution obtained applies exactly to the case where a symmetry exists with respect to the plane of the constriction. Using equation (13) it can be shown that the

exact flux distribution at the constriction would be,

$$q = -k \left( \frac{\partial T}{\partial y} \right)_{y=0}$$

or

$$q = \frac{H \cos\left(\frac{\pi x}{2a}\right)}{2a \sqrt{\sin^2\left(\frac{\pi b}{2a}\right) - \sin^2\left(\frac{\pi x}{2a}\right)}} \dots\dots\dots (54)$$

According to this equation, the flux distribution at the constriction is a function of the channel dimension as well as the constriction dimension. If  $b \ll a$ , and hence  $x \ll a$ , equation (53) becomes a special case of equation (54).

From Fig. 7 it can be seen that there is a very good agreement between the present experiments and theory. The experimental points of Kouwenhoven and Sackett also agree very well with the present theory, with the exception of the point corresponding to  $C = 0.5$ . The divergence there could have been produced by the errors introduced due to the finite constriction neck. Any such error should be large for high values of  $C$ , since the constriction neck resistance would then be large as compared with the constriction (spreading) resistance. It is noteworthy that the experimental points of Kouwenhoven and Sackett are in better agreement with the present theory than their theory, although the angle  $\theta$  of their theory was so selected as to give the best fit with the experiments.

#### Eccentric Constrictions

The results of the present investigation and reference (5) are plotted in Figs. 8, 9 and 10 as the ratio of the conduc-

tance number to that of zero eccentricity  $U/U_0$  versus the eccentricity number  $E$  for the constriction numbers of 0.125, 0.08 and 0.04 respectively. The experimental points are those of the present experiments ( $C=0.125$ ) and those of Sackett<sup>(5)</sup> ( $C=0.08$  and  $C=0.04$ ) who used metallic specimens with finite constriction necks and electrical analogy in his experiments. The theoretical curves were obtained from the present theory using the appropriate values of the constriction number  $C$  and also from a relationship derived by Sackett. In his theory, Sackett employed the same wedge model described earlier and obtained a relationship for the ratio of the resistance increase due to eccentricity to the constriction resistance for zero eccentricity. In terms of the present dimensionless numbers, it can be written as,

$$\frac{U}{U_0} = \frac{\ln\left(\frac{1}{C}\right) + C - 1}{\ln\left\{\frac{1}{C(1-E+EC)}\right\} - (1+E)(1-C)} \dots\dots\dots (55)$$

Since a function (tangent) of the wedge angle  $\theta$  enters the resistance (or conductance) relationship as a product, in the conductance ratio  $U/U_0$  they cancel out and the ratio becomes independent of the wedge angle selected.

From Figs. 8, 9 and 10, it can be seen that the agreement between the experiments and both the theories is good at or near the extreme values of the eccentricity number, i.e.,  $E=0$  and  $E=1$ . However, in the region between the extreme values of  $E$ , the present theory's agreement with the experiments is much better.

### Conclusion

One closed form equation is derived for calculating the exact thermal conductance of two-dimensional symmetrical constrictions, and an infinite series equation for the thermal conductance of two-dimensional eccentric constrictions. The agreement between the theory and experiments for both cases is good. Thermal conductance of two-dimensional constrictions increase with (a) increase in thermal conductivity, (b) increase constriction width, (c) decrease in channel width, and (d) decrease in eccentricity.

### Acknowledgements

The research reported in this paper was carried out under the sponsorship of the National Aeronautics and Space Administration, under Grant NGR 10-007-010. The assistance of Mr. J. D. Patel and Mr. M. Sniad, both of the University of Miami, is gratefully acknowledged.

References

1. Gex, E. D., "Thermal Resistance of Metal-to-Metal Contacts - An Annotated Bibliography", ASTIA Document 263181, July 1961.
2. Atkins, H.L., "Bibliography on Thermal Metallic Contact Conductance", NASA Marshall Space Flight Center, NASA - TM-X-53227, 26 pp, April 1965.
3. Vidoni, C. M., "Thermal Resistance of Contacting Surfaces: Heat Transfer Bibliography", University of California, Lawrence Radiation Laboratory, UCRL-14264, AEC Contract No. W-7405-Eng.-48, June 1965.
4. Kouwenhoven, W. B., and Sackett, Jr., W. T., "Electrical Resistance Offered to Non-uniform Current Flow", Welding Research Supplement, pp. 466s-470s, October 1949.
5. Sackett, Jr., W. T., "Contact Resistance", Ph.D. Dissertation, The Johns Hopkins University, 1950.
6. Mikic, B. B., and Rohsenow, W. M., Appendix D, "Thermal Contact Resistance", M.I.T., Heat Transfer Laboratory Report No. DSR 74542-41, Contract No. NGR-22-009-065, September 1966.

Nomenclature

Symbols

A	Cross-sectional area of flow channel
a	Half width of Heat Flow Channel
B	Constant
b	Half width of Constriction
C	Constriction Number ( $=b/a$ )
E	Eccentricity Number ( $=e/(a-b)$ )
e	Eccentricity
H	Heat flow rate
i	$\sqrt{-1}$
k	Thermal conductivity
L	Flow channel length; Distance between voltmeter probes
ln	Natural logarithm
m	Proportionality factor; Temperature slope away from constriction
O	Origin; Point in flow channel boundary
P	Point in flow channel boundary
q	Thermal flux
Q	Point in flow channel boundary
R	Resistance; Point in flow channel boundary
S	Point in flow channel boundary
T	Temperature
t	Flow channel thickness
U	Conductance Number ( $=2au/k$ )
u	Abscissa in complex w plane; Constriction conductance per unit area
v	Ordinate in complex w plane
w	Complex plane
X	Abscissa in complex Z plane
x	Abscissa in two-dimensional plane; Abscissa in complex z plane
Y	Ordinate in complex Z plane

Symbols

Y	Ordinate in two-dimensional plane, Ordinate in complex z plane
Z	Complex plane
z	Complex plane
$\Delta$	Difference
$\theta$	Angle
$\rho$	Resistivity

Subscripts

c	Constriction
m	Mean
n	Number
o	No-constriction

List of Figures

- Fig. 1. - Various Cases Illustrating Two-Dimensional Constriction of Heat Flow.
- Fig. 2. - Heat Flow Lines and Isotherms in Two-Dimensional Symmetrical Constriction.
- Fig. 3. - Transformation From Linear Heat Flow to Heat Flow with Constriction in a Semi-Infinite Slab.
- Fig. 4. - Two-Dimensional Eccentric Constriction.
- Fig. 5. - Specimens Used in Experiments for Studying Two-Dimensional Constriction Conductances.
- Fig. 6. - Experimental Set-up for Studying Two-Dimensional Constriction Conductances.
- Fig. 7. - Experimental and Theoretical Relationships Between Conductance Number and Constriction Number for Two-Dimensional Symmetrical Constrictions.
- Fig. 8. - Experimental and Theoretical Relationships Between Conductance Ratio and Eccentricity Number for  $C=0.125$ .
- Fig. 9. - Experimental and Theoretical Relationships Between Conductance Ratio and Eccentricity Number for  $C=0.08$ .
- Fig. 10.- Experimental and Theoretical Relationships Between Conductance Ratio and Eccentricity Number for  $C=0.04$ .

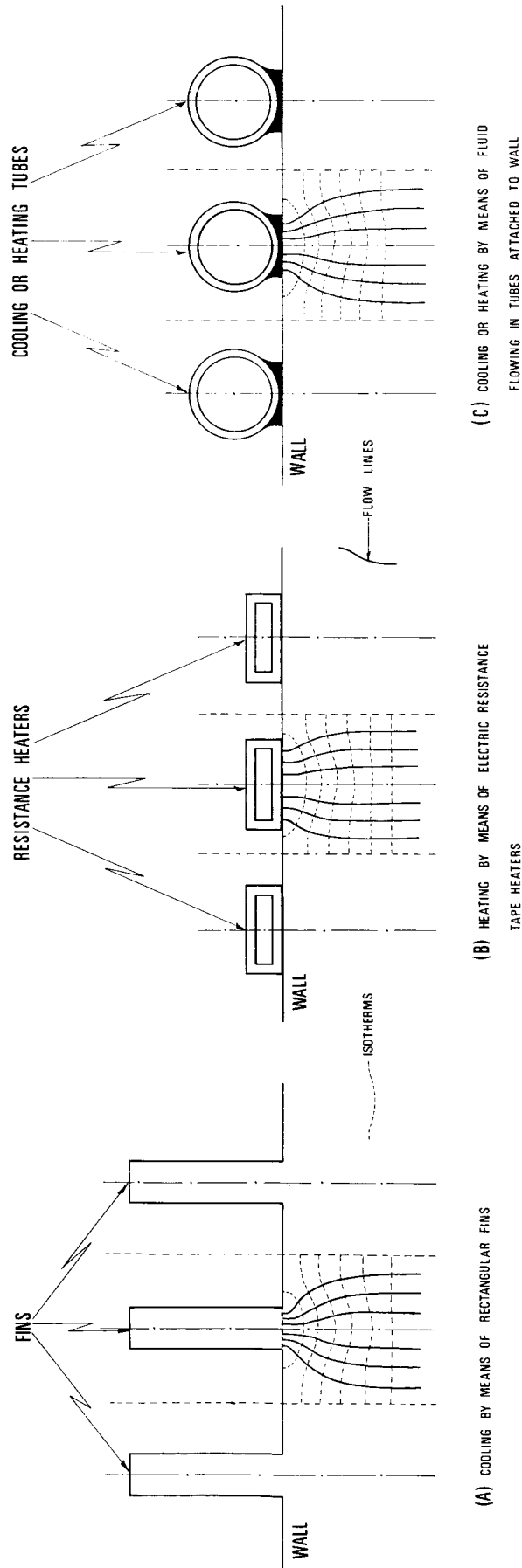
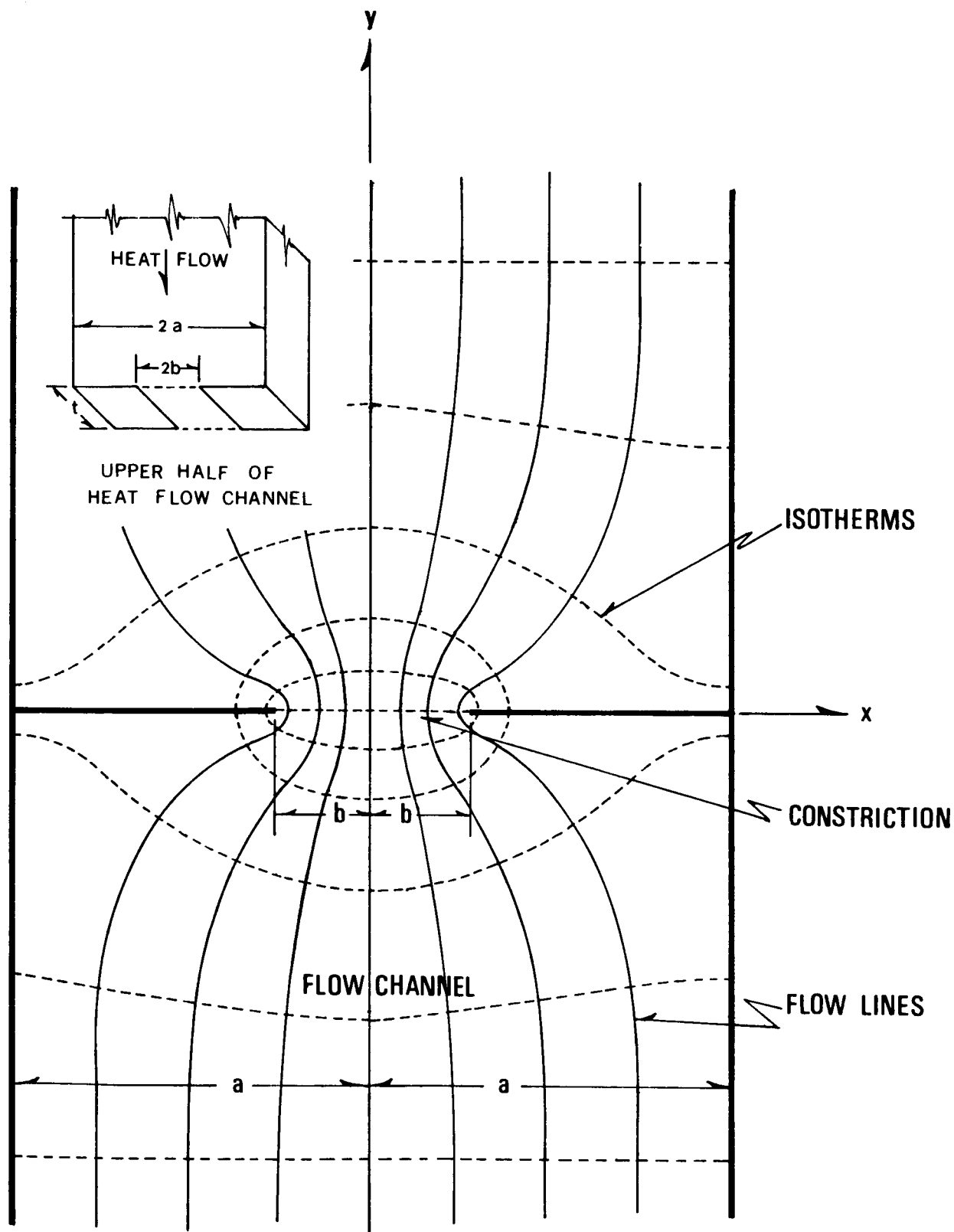
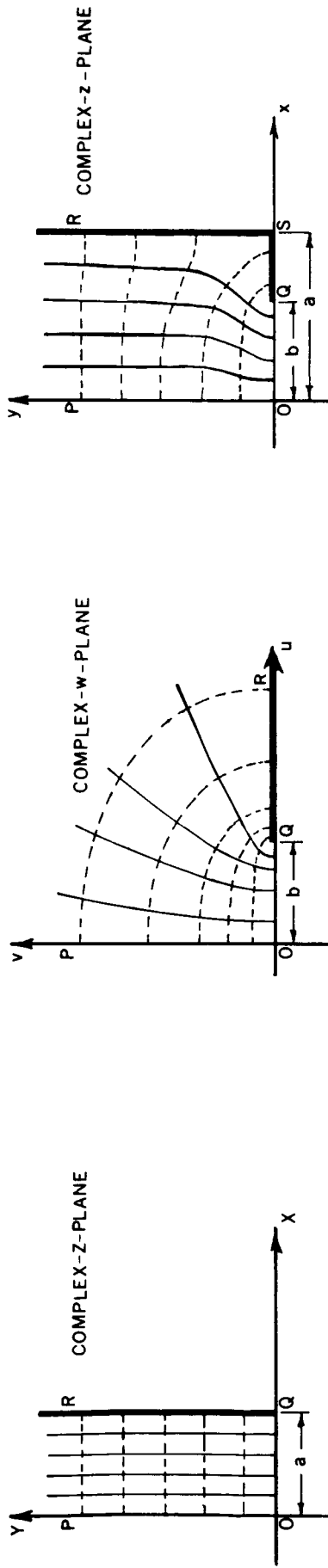


FIG.1. VARIOUS CASES ILLUSTRATING TWO DIMENSIONAL CONSTRICTION OF HEAT FLOW



**FIG.2. HEAT FLOW LINES AND ISOTHERMS IN TWO DIMENSIONAL SYMMETRICAL CONSTRICTION**

HEAT FLOW LINES: \_\_\_\_\_ ISOTHERMS: - - - - -



(A) LINEAR HEAT FLOW IN A SEMI-INFINITE SLAB  
 (B) HEAT FLOW IN A SEMI-INFINITE SOLID THROUGH A RECTANGULAR OPENING  
 (C) HEAT FLOW IN A SEMI-INFINITE SLAB HAVING A CUT

FIG. 3.- TRANSFORMATION FROM LINEAR HEAT FLOW TO HEAT FLOW WITH CONSTRICTION IN A SEMI-INFINITE SLAB

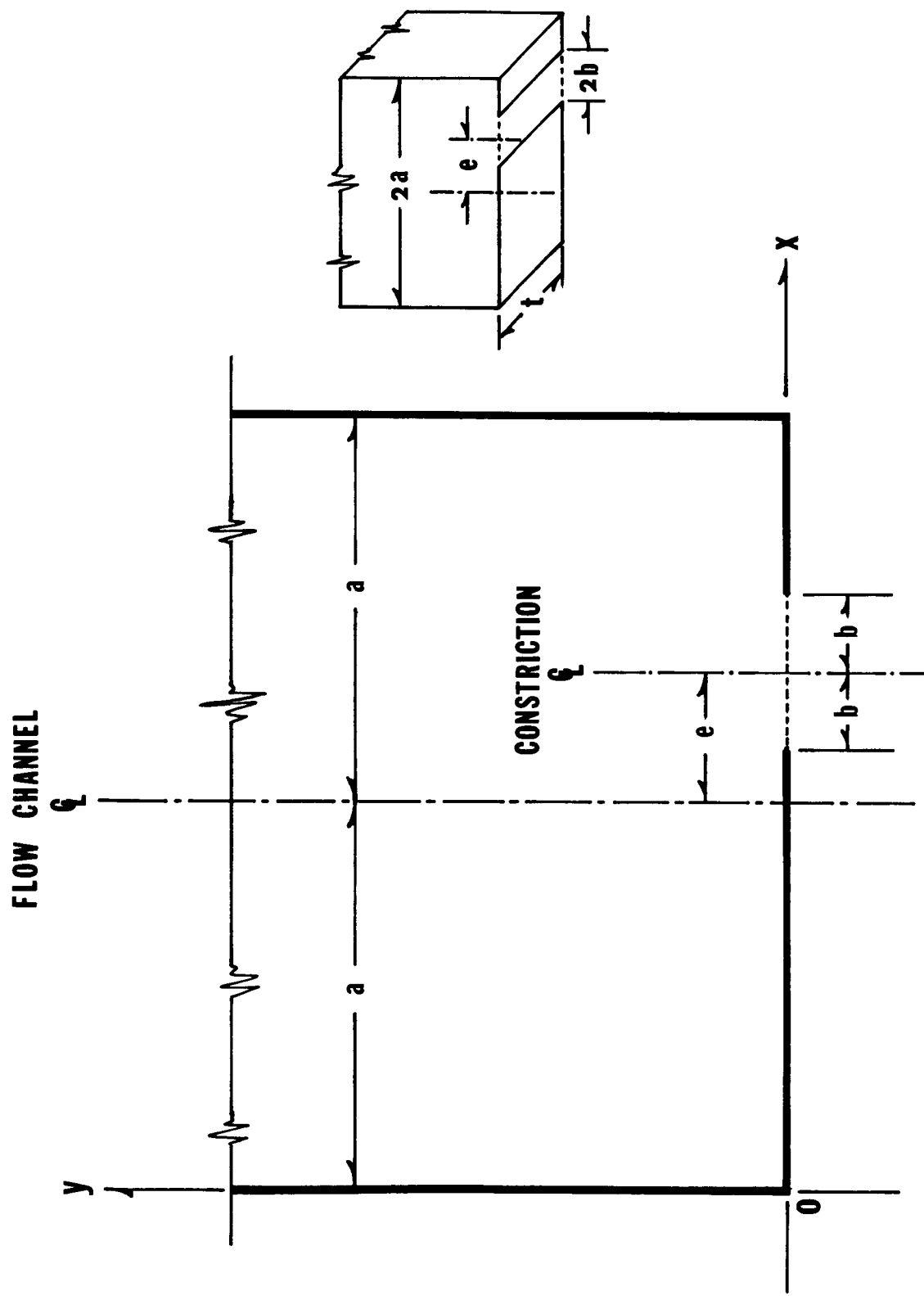
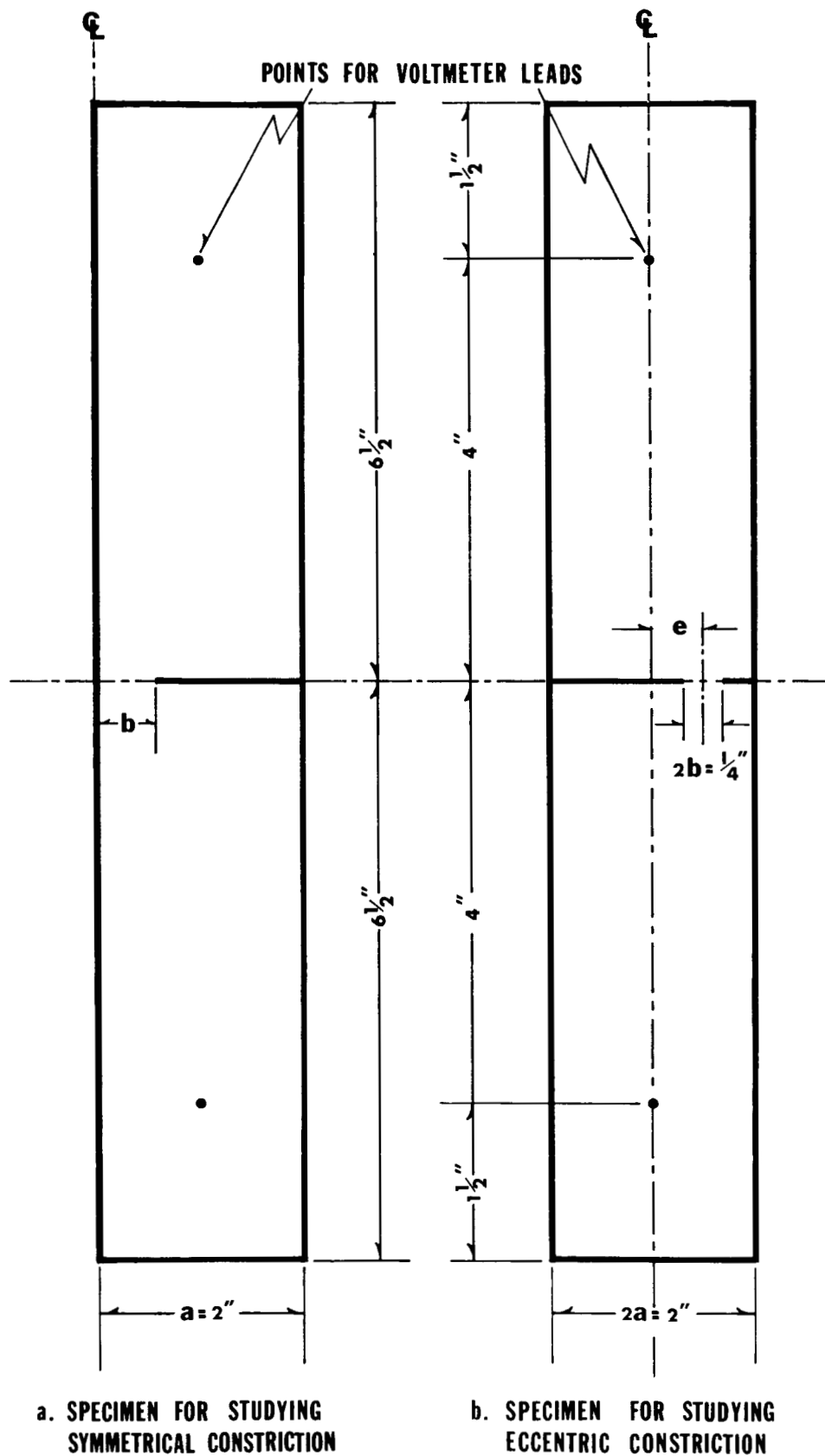
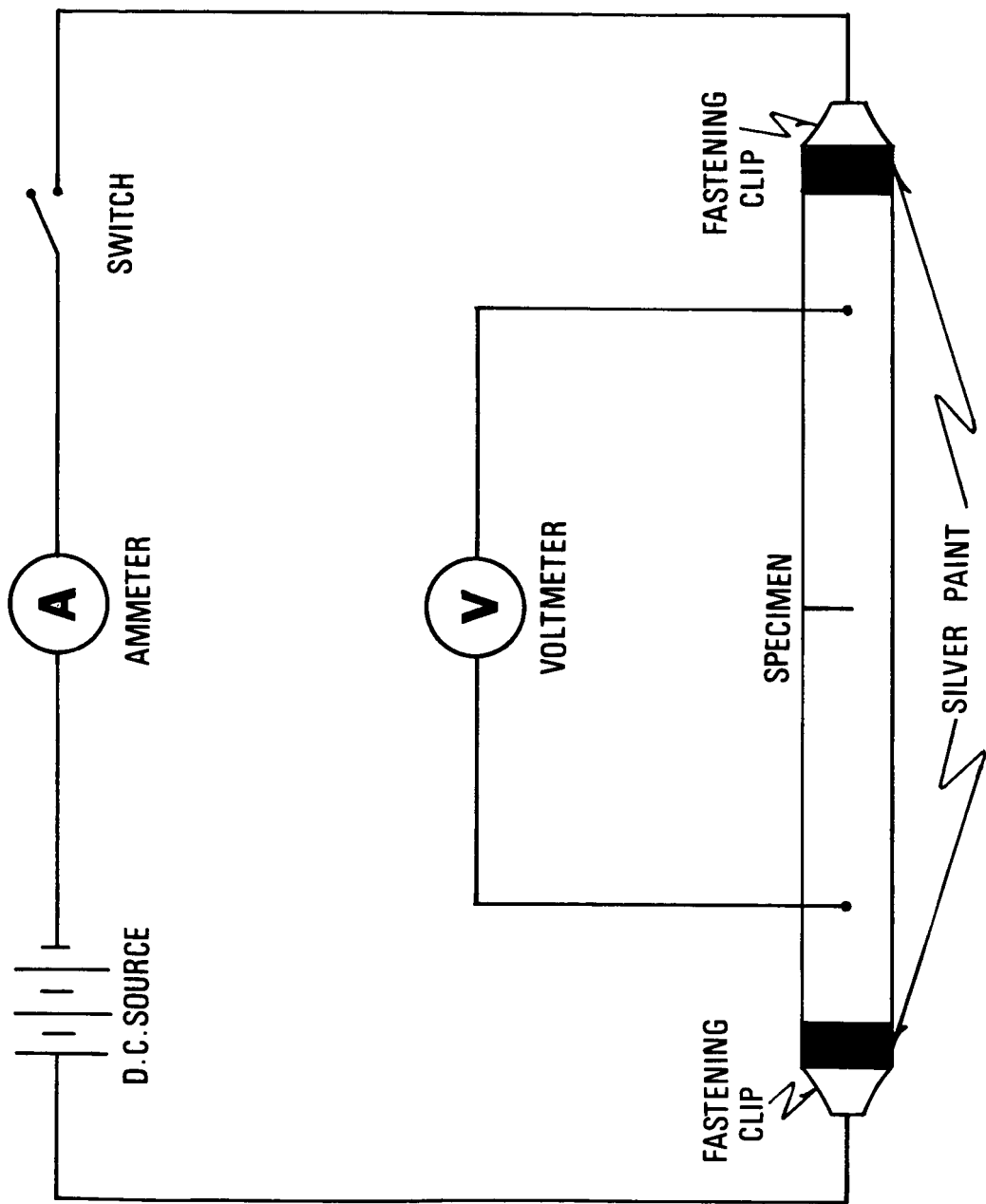


FIG.4. TWO DIMENSIONAL ECCENTRIC CONSTRICTION



**FIG.5. SPECIMENS USED IN EXPERIMENTS FOR STUDYING TWO DIMENSIONAL CONSTRICTION CONDUCTANCES**



**FIG.6. EXPERIMENTAL SET-UP FOR STUDYING TWO DIMENSIONAL  
CONSTRICION CONDUCTANCES**

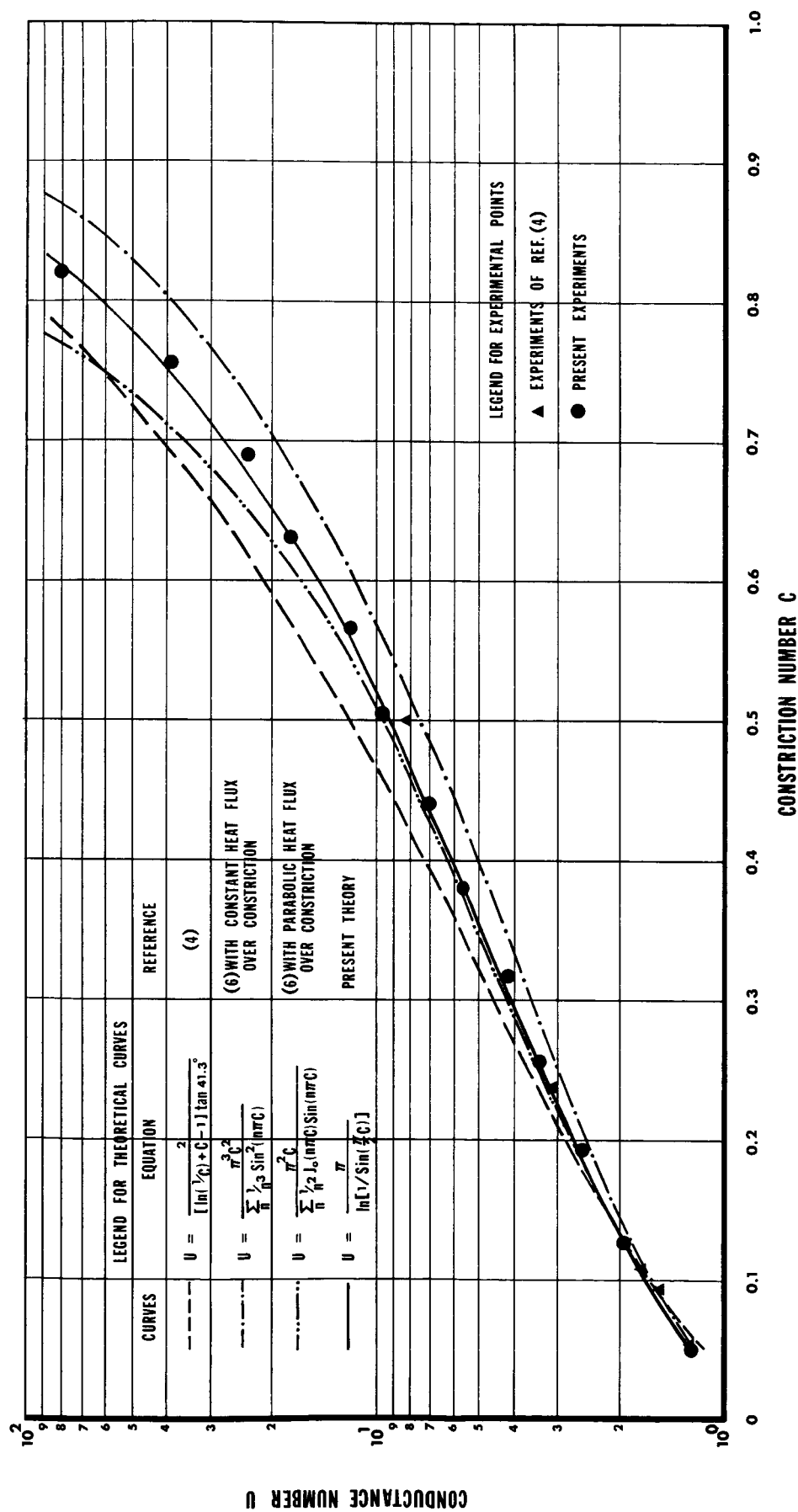
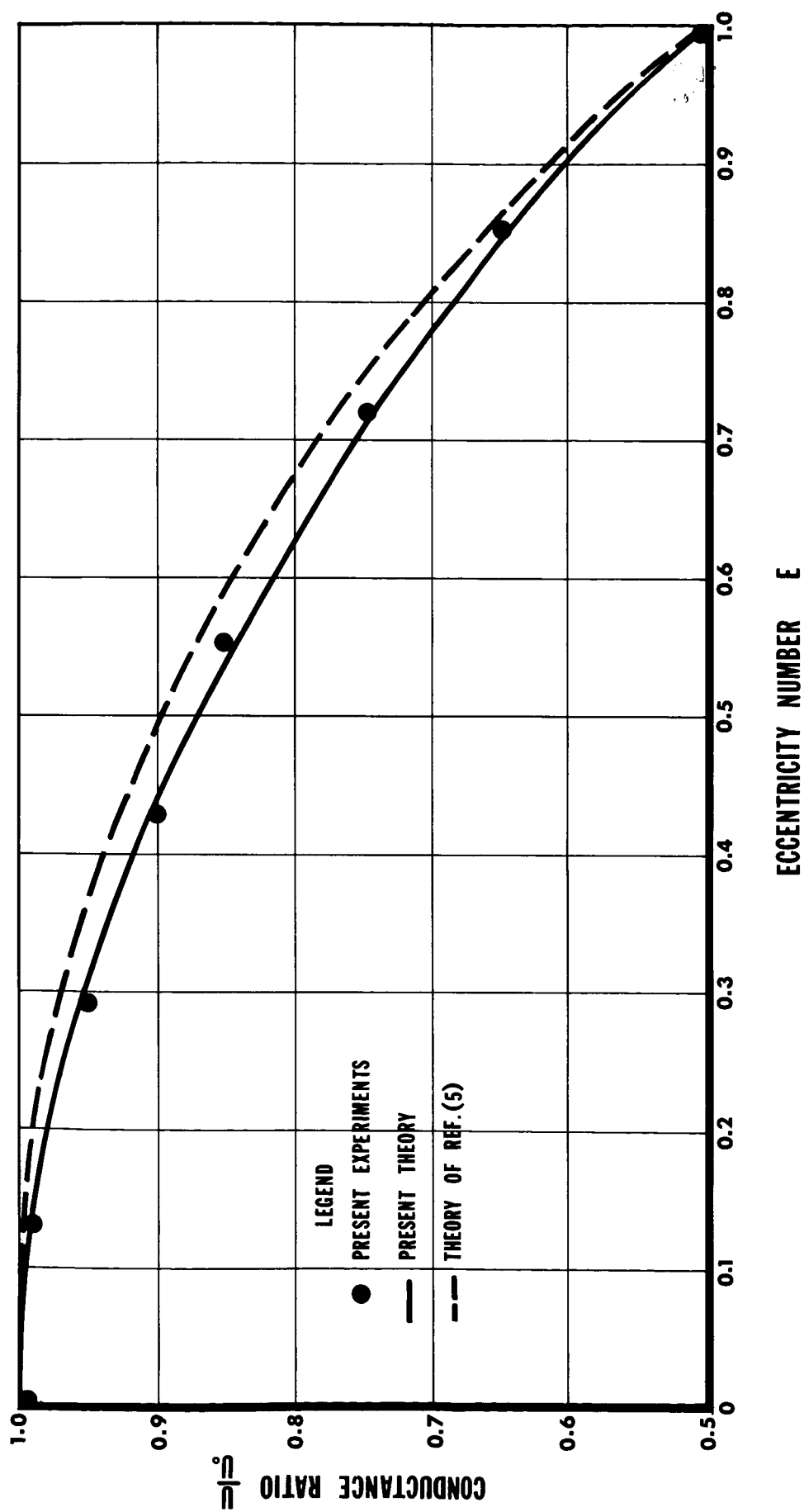
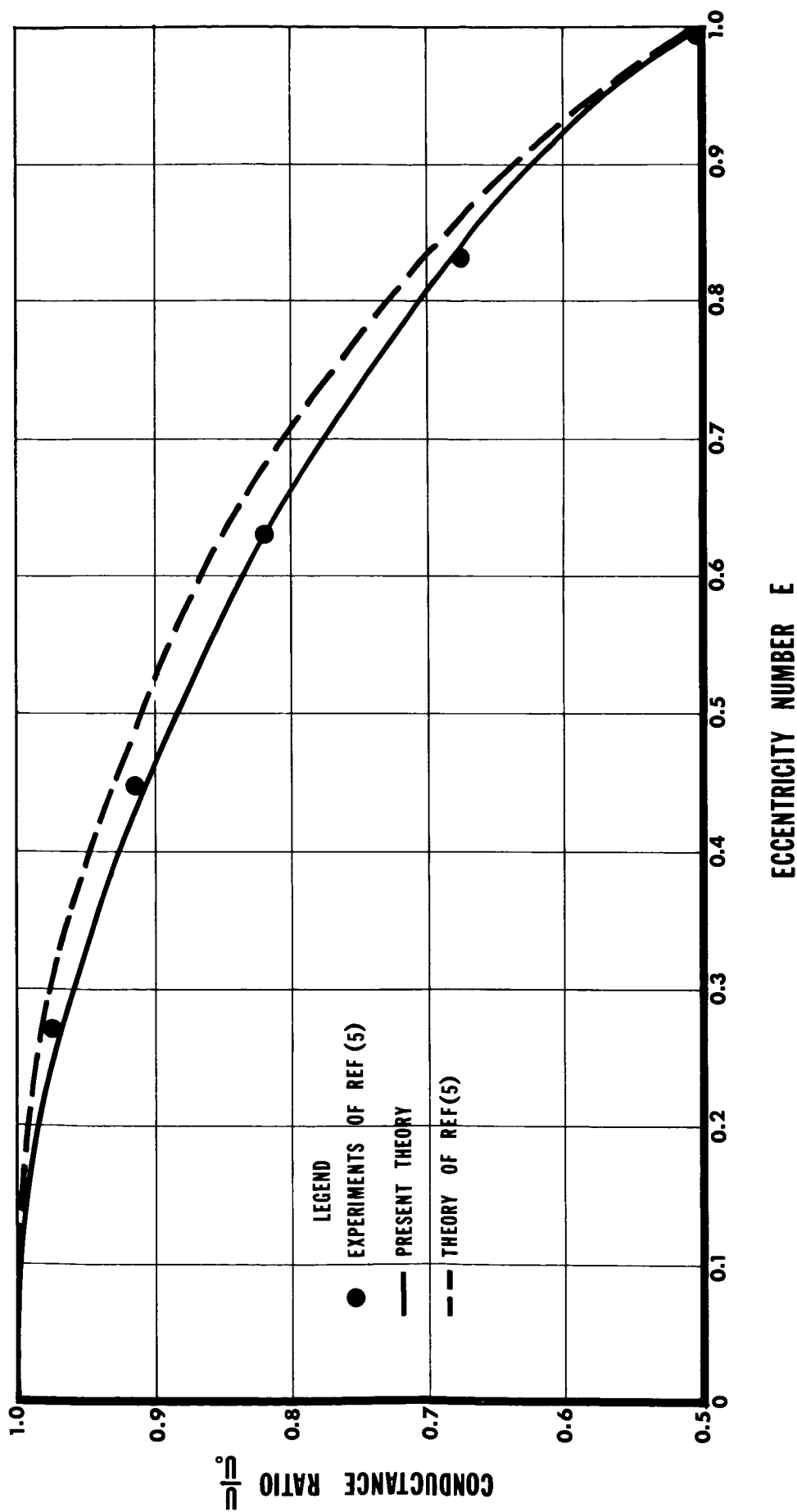


FIG. 7. EXPERIMENTAL AND THEORETICAL RELATIONSHIPS BETWEEN CONDUCTANCE NUMBER AND CONSTRICTION NUMBER FOR TWO DIMENSIONAL SYMMETRICAL CONSTRICTIONS



**FIG.8. EXPERIMENTAL AND THEORETICAL RELATIONSHIPS BETWEEN CONDUCTANCE RATIO AND ECCENTRICITY NUMBER FOR  $C = 0.125$**



**FIG.9. EXPERIMENTAL AND THEORETICAL RELATIONSHIPS BETWEEN CONDUCTANCE RATIO AND ECCENTRICITY NUMBER FOR C=0.08**

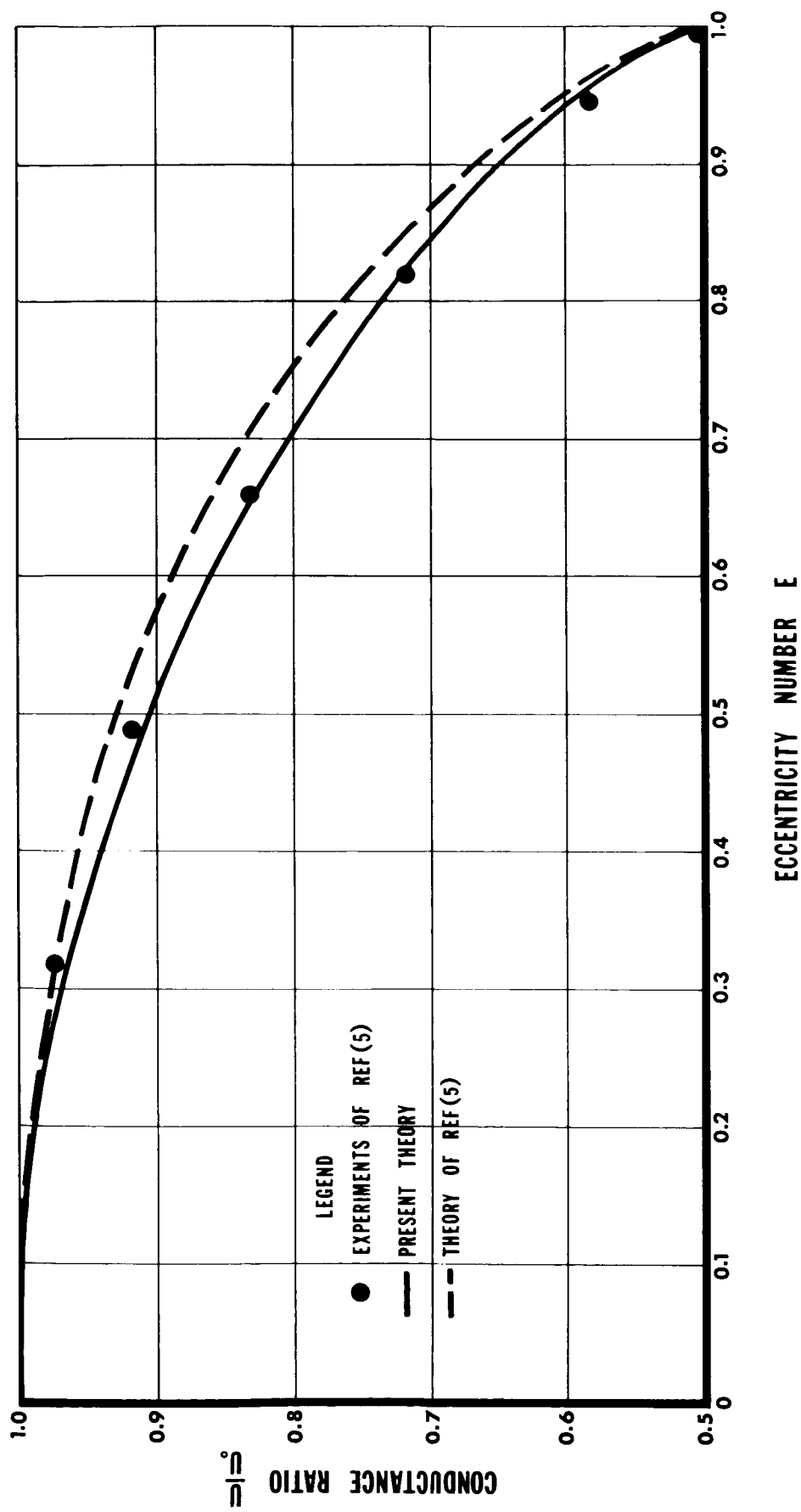


**FIG.10. EXPERIMENTAL AND THEORETICAL RELATIONSHIPS BETWEEN CONDUCTANCE RATIO AND ECCENTRICITY NUMBER FOR C=0.04**